www.czasopisma.pan.pl PAN POLSKA AKADEMIA NAUK www.journals.pan.pl

Arch. Metall. Mater. **63** (2018), 1, 87-97

DOI: 10.24425/118913

A.N. WIECZOREK*#, A. STACHOWIAK**, W. ZWIERZYCKI**

EXPERIMENTAL DETERMINATION OF THE SYNERGISTIC COMPONENTS OF TRIBOCORROSIVE WEAR OF Ni-Cu-Mo-AUSFERRITIC DUCTILE IRON

The paper presents results of a two-stage study on the tribocorrosive wear of ADI alloy cast iron containing Ni and Cu. In the first stage of the wear tests with use test rig type pin-on-plate, there were determined the parameters of the process of tribocorrosion of the ADI cast iron in 3.5% NaCl solution. In the second stage, the tests were carried out on a test rig simulating real operating conditions of chain wheels used in armoured face conveyors. The purpose of this study was to demonstrate the impact of the combined action of corrosive agents (water and NaCl) and quartz abrasive on the wear of the wheels tested. As part of the test, the abrasive wear in the presence of the abrasive material alone and in the presence of a mixture of the abrasive material, water and NaCl was determined. The microstructure and the hardness of the surface layer as a function of the distance from the surface were also determined. During the study it has been found that regardless of the type of test there is a synergy between the effects of corrosion and friction which led to an increase of the resulting wear by 30%.

Keywords: ADI, tribocorrosion, wear

1. Introduction

At present, the most important problems determining the further development of the methods of forecasting the tribocorrosive wear include the experimental and analytical identification of probable wear mechanisms in the entire available space of operating excitations as well as the preparation of formulas for calculating the effects (i.e. wear) of those different processes. This study constitutes the first stage in achieving this comprehensive goal (experimental cognition) in a situation where the wear of the components is determined also by the abrasive material and the aggressive corrosive medium in addition to mechanical excitations.

In the case of friction pairs of machines, the wear of individual elements often occurs as a result of a simultaneous action of friction and corrosion – i.e. tribocorrosion. Tribocorrosion is a wear process caused by the simultaneous action of mechanical excitations and corrosive environmental factors [1-5] which generally constitutes a significant operational problem. Tribocorrosive wear occurs most often in tribological systems composed of two or three bodies that move in relation to each other. In the real conditions, where friction and electrochemical processes occur at the same time, there is observed a synergistic effect of the impact of the both processes which significantly greater than the sum of their individual impacts [6,7].

The essence of the process is the removal of the protective layer of passive oxides or the disruption of its continuity by the action of mechanical factors (e.g. hard abrasive) which results in its restoration in the form of a new layer of passive oxides on the exposed surface as a consequence of electrochemical process. The removal of the passive layer of oxides caused by tribological processes accelerates the corrosion, because there takes place a rapid digestion of the surface underlying the layer that has been removed. Another factor intensifying the tribocorrosive wear is intense abrasive action of hard particles coming from the oxide layers being removed. Processes of removing and restoring the oxide layers occur cyclically along with each action of a mechanical factor. The intensity of tribocorrosion depends primarily on the characteristics of the materials, of which the elements of the friction pairs are made, as well as on the conditions of excitations [1].

Currently, a number of industries, particularly those related to power engineering and mineral extraction, use machines and equipment at risk of damage due to abrasive wear and tribocorrosive wear [8,9]. This issue is particularly important considering the sustainable development of the industry which assumes conservation of energy and natural resources [10]. An example of elements subjected to a combined action of mechanical factors (abrasive grains) and corrosive factors are chain wheels of armoured face conveyors (Fig. 1) which are used for example in coal handling systems of power plants and combined heat and power plants, as well as in underground, surface and tunnel mining. Armoured face conveyors are often used for transport of mineral and energy resources. During the transport, hard grains of these materials and aqueous electrolyte solutions penetrate

* SILESIAN UNIVERSITY OF TECHNOLOGY, INSTITUTE OF MINING MECHANIZATION, 44-100 GLIWICE, POLAND
** POZNAŃ UNIVERSITY OF TECHNOLOGY, INSTITUTE OF MACHINES AND MOTOR VEHICLES, 5 MARII SKŁODOWSKIEJ-CURIE SQ., 60-965 POZNAŃ, POLAND
# Corresponding author: andrzej.n.wieczorek@polsl.pl

to the zone of mating between the driving wheel and the chain (Fig. 2). In [11], based on an analysis of the operational damage to chain drums of armoured face conveyors, it has been estimated that the abrasive and tribocorrosive wear accounted for over 45% of the damages leading to removal of chain drums of armoured face conveyors from service.

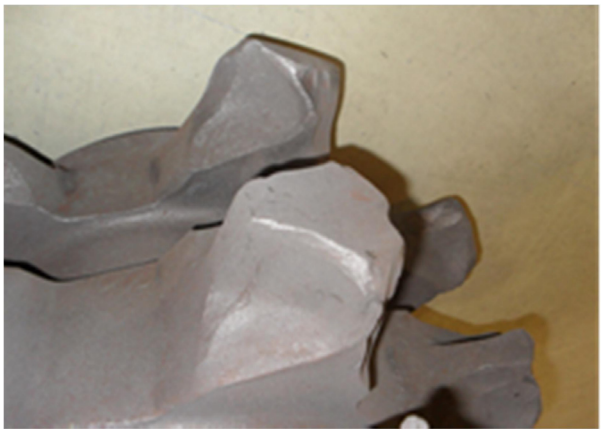

Fig. 1. An example view of tribocorrosive wear of a chain wheel in an armoured face conveyor

Fig. 2. An example view of a fragment of an armoured face conveyor with sand and water contamination in the discharge zone

Manufacturers and users have high expectations associated with the use of ADIs which offer a number of advantages [12,13] as compared with surface hardened alloy steels. One of the most important factors predisposing these materials for the use in harsh operating conditions is that ADIs are resistant to wear almost in the entire cross section of the cast.

Austempered ductile irons are used as materials for machines operating in harsh operating conditions, although their use is not very widespread. This may result from a complex technology used in the production of these materials, which is characterized by the necessity of determining a large number of parameters affecting their functional properties. It should however be noted that there are almost no studies on operating properties of the corrosive and abrasive factors with respect to ADIs, in particular on their synergistic action, which could have also affect the decisions of users as to the use of these cast irons.

Advantageous performance characteristics of austempered ductile iron are observed after properly conducted heat treatment that consists of austenitization and isothermal quenching. The conditions of the austenitization process determine the content of carbon in austenite, while the parameters of the „process window" of the isothermal transition shape ultimately the ausferritic microstructure composed of bainitic ferrite and austenite. The combination of parameters of the isothermal transition temperature and the process duration is important for the diffusion of carbon into austenite and its further stabilization.

A characteristic feature of ADIs is their ability to strengthen as a result of the phase transition of austenite into strain-induced martensite caused by an increase in the stress or strain [14]. A number of authors, including Hayrynen et al. [12,13], Schissler at al. [15], Owhadi at al. [16], Myszka and Wieczorek [17,18] confirmed a positive impact of the phase transition on wear properties of ADIs.

Corrosion properties of the austempered ductile irons were analysed in a number of research studies. Prasanna et al. [19] reported a loss of mass by approx. 33% caused by corrosion (for ductile iron after austempering as compared with the same ductile iron without heat treatment). Hsu and Chen [20] tested nodular cast irons and ADIs in the presence of 3.5% NaCl solution and confirmed an improved resistance of cast irons to corrosion after isothermal quenching and a favourable effect of 4% nickel content on anti-corrosive properties. Banerjee et al. [21] have found that an increase in the amount of graphite inclusions in the structure of ADIs increased the rate of the corrosion wear and that the copper content had a favourable effect on an increase in the corrosion resistance of these cast irons. Hsu and Lin [22] also demonstrated a favourable effect of copper on the corrosion resistance of ADIs, but they conducted their tests on cast irons containing 1% of Cu.

Cai eta al. [23] examined the resistance of ADIs to fatigue damage depending on the ambient humidity and they found that this resistance was lower in an atmosphere containing water. As a reason for this phenomenon they indicated the formation of corrosion pits in graphite inclusions, which initiated local cracks of the ADI matrix. Krawiec et al. [24] found dependence between the corrosion resistance and the microstructure of ADI. In particular they showed that the microstructure of upper ausferrite had a higher resistance as compared with lower ausferrite. Myszka et al. [25] demonstrated the possibility of increasing the corrosion resistance of ADIs by simultaneous austenitizing and nitriding or austenitizing and carbonitriding.

2. Synergetic components of the tribocorrosive wear process

The main purpose of this study was to identify the manner of wear of ADIs containing Ni, Cu and Mo in conditions of simultaneous action of friction and corrosion in a sliding pair. The authors focused particularly on assessing the effect of synergy between the mechanical and corrosive impacts. It has been assumed that this objective will be achieved through laboratory tests and controlled operating tests reproducing the real conditions of operation of the chain wheels.

In the case of the laboratory tests, it has been assumed that the total loss of the material Vt in complex conditions of excitations will be the sum of the following elementary components [7,26-29]:

$$V_t = V_f + V_{corr} + \Delta V \tag{1}$$

where:

V_f – wear caused by friction (without the participation of corrosion),

V_{cor} – corrosive wear only (without the participation of friction),

ΔV – summary effect of the synergy of friction and corrosion.

The ΔV factor characterizing the effect of synergy of friction and corrosion can be determined by the following relationship:

$$\Delta V = \left(\Delta V_f + \Delta V_{cor}\right) \tag{2}$$

where:

ΔV_f – increase in the wear resulting from the synergistic effect of corrosion on friction,

ΔV_{cor} – increase in the wear resulting from the synergistic effect of friction on corrosion.

After taking into account the relationship (2), the equation (1) will take the following form:

$$V_t = \left(V_f + \Delta V_f\right) + \left(V_{cor} + \Delta V_{cor}\right) \tag{3}$$

Equation (3) allows determining the increase in the wear associated with the synergistic effect of corrosion on friction in the following form:

$$\Delta V_f = V_t - \left(V_f + V_{cor} + \Delta V_{cor}\right) \tag{4}$$

One of the most effective methods of estimating the wear component resulting from friction (V_f) is to conduct tests in a corrosive environment in the conditions of cathodic polarization [26,27]. The cathodic polarization ensures protection of the material against aggressive action of the environment. At the same time, the test conditions take into account the impact of the electrolyte as a substance lubricating and cooling the friction pair. The method described constitutes a more reliable manner of estimating the wear component resulting from friction (V_f) than examining the loss of the material during dry sliding friction [7].

The wear component resulting exclusively from the corrosive action of the environment can be determined based on the Faraday equation for the corrosion current density (icor). The corrosion current density is determined by approximating the polarization curve with the use of Tafel equations. This method can be used to estimate the sum of the components ($V_{core} + \Delta V_{cor}$) [27,29]. The polarization curve determined for the conditions of the wear test should be used for this purpose. Consequently, the ΔV_{cor} component can be determined from the formula:

$$\begin{aligned}\Delta V_{cor} &= \left(V_{cor} + \Delta V_{cor}\right) - V_{cor} = \\ &= f\left(i_{cor\_without\_wear}\right) - f\left(i_{cor\_with\_wear}\right)\end{aligned} \tag{5}$$

In order to estimate the effect of the synergy between abrasive and corrosive impacts taking place in the case of operating tests that reproduce real conditions of operation of the chain wheels, it has been assumed that the total material loss $V_{ABR+COR}$ will be determined in the same way as in the equation (3), using the sum of the following elementary components:

$$V_{ABR+COR} = \left(V_{ABR_f} + \Delta V_{ABR_f}\right) + \left(V_{ABR_{cor}} + \Delta V_{ABR\_cor}\right) \tag{6}$$

where:

V_{ABR_f} – wear caused by frictional impact of the abrasive (without the participation of corrosion),

V_{ABR_cor} – corrosive wear in the presence of stationary abrasive,

ΔV_{ABR_f} – increase in the wear resulting from the synergistic effect of the corrosion products on the composition of the abrasive,

ΔV_{ABR_cor} – increase in wear resulting from the synergistic effect of the abrasive on corrosion.

For the purpose of determining the value of the component ΔV_{ABR_f}, it has been assumed that the ratio of the value of the wear component resulting from the corrosive impact V_{cor} and the total loss of the material V_t is equal to the ratio of component of the corrosive wear in the presence of stationary abrasive V_{ABR_cor} and the total material loss $V_{ABR+COR}$:

$$\frac{V_{cor}}{V_t} = \frac{V_{ABR\_cor}}{V_{ABR+COR}} \tag{7}$$

Therefore, V_{ABR_cor} can be determined from:

$$V_{ABR\_cor} = \frac{V_{cor}}{V_t} \cdot V_{ABR+COR} \tag{7a}$$

In addition it has assumed that the ratio of the sum of the wear component resulting from the corrosive action V_{cor} and the increase in the wear resulting from of the synergistic effect of the friction on corrosion ΔV_{cor} to the total wear V_t is equal to the ratio of the sum of the corrosive wear component in the presence of the stationary abrasive V_{ABR_cor} and the increase in the wear resulting from the synergistic effect of the abrasive on corrosion ΔV_{ABR_cor} to the total material loss $V_{ABR+COR}$. This can be described by the following relationship:

$$\frac{\left(V_{cor} + \Delta V_{cor}\right)}{V_t} = \frac{\left(V_{ABR\_cor} + \Delta V_{ABR\_cor}\right)}{V_{ABR+COR}} \tag{8}$$

After the transformation in relation to the sum (V_{ABR_cor} + ΔV_{ABR_cor}), the equation (8) takes the following form:

$$\left(V_{ABR\_cor} + \Delta V_{ABR\_cor}\right) = \left(\frac{\left(V_{cor} + \Delta V_{cor}\right)}{V_t}\right) \Delta V_{ABR+COR} \tag{9}$$

The assumptions adopted can be substantiated by the same chemical composition of the sample tested using the laboratory method and the chain wheel used for operating tests, nearly identical electrochemical potential of the electrolyte used for

both tests, as well as an inconsiderable influence of quartz on the electrochemical properties of the corrosion system. The increase in the wear resulting from the synergistic effect of the abrasive on the corrosion ΔV_{ABR_cor} can be described by a relationship similar to the equation (5):

$$\Delta V_{ABR\_cor} = \left(V_{ABR\_cor} + \Delta V_{ABR\_cor}\right) - V_{ABR\_cor} \tag{10}$$

Using the equation (8), the increase in the wear resulting from the synergistic effect of corrosion products on the abrasive ΔV_{ABR_f} can be determined with the use of the following relationship:

$$\Delta V_{ABR\_f} = V_{ABR+COR} - \left(V_{ABR\_f} + \frac{V_{cor} + \Delta V_{cor}}{V_t} \Delta V_{ABR+COR}\right) \tag{11}$$

The summary synergy effect of abrasive and corrosive impacts ΔV_{ABR} results from the relationship:

$$\Delta V_{ABR} = \Delta V_{ABR\_f} + \Delta V_{ABR+COR} \tag{12}$$

3. Experimental details

3.1. Characteristics of the tested ADI

The input material for the production of ADI_360 was EN-GJS-600-3 (PN-EN 1563) ductile iron with the composition presented in Table 1.

TABLE 1

Chemical composition of ductile iron EN-GJS-600 [mass%]

C	**Si**	**Mn**	**S**	**P**
3,50	2,54	0,16	0,013	0,041
Mg	**Cr**	**Cu**	**Ni**	**Mo**
0,047	0,026	0,50	1,40	0,24

The ductile iron castings had a pearlitic-ferritic structure with the graphite nodule count of 200 per 1 mm^2, while the spheroidization of graphite was greater than 90%. After the final material removal processing the ductile iron castings were subjected to a heat treatment in order to obtain an austempered structure typical of ADIs. The parameters of heat treatment in a salt bath used for the wheels under consideration are shown in Table 2, while the mechanical properties obtained – in Table 3.

TABLE 2

List of the process parameters used in the production of ADI_360 cast iron

Heat treatment parameters	**ADI_360**
Austenitising temperature, °C	950
Austenitising time, min	180
Austempering temperature, °C	360
Austempering time, min	150

TABLE 3

Mechanical properties of the ADI tested

Mechanical Properties	**ADI_360**
Tensile Strength TS, MPa	1028
Yield Strength YS, MPa	652
Impact Toughness K, J	124
Elongation A5, %	10

3.2. Laboratory test rig and methods

The wear tests were performed on a pin-on-plate test rig. A detailed description of the test rig and the test methods is presented in [30,31]. The pair used as a model is a hard, non-deformable pin which slides in a reciprocating manner on the surface of the sample. The following elements were used in the tests:

- a pin made of cemented carbide (WC) coated with a layer of titanium nitride (TiN); the pin has the shape of a truncated cone with an apex angle of 70°; the diameter of the flat end is 0.5 mm; the average hardness is approx. 2000 HV.
- samples of the cast iron in the shape of a cube with the edge of 10 mm.

A three-electrode system with a precise four-channel ATLAS 9833 potentiometer was used for the studies on electrochemical phenomena. A saturated calomel electrode(SCE) was used as the reference electrode. The auxiliary electrode was a platinum mesh.

During the tests, the pin moved on a distance of approx. 6 mm with a frequency of 5 Hz. All the tests were performed at a pressure of 45 MPa. For given conditions of excitations, at least 3 research tests consisting of 54,000 movements of the pin were carried out.

The wear of sample surfaces was evaluated after completion of the test. As a measure of the wear there was adopted the depth of the wear trace determined by the profilometry measurements in the direction perpendicular to the contact surface at the half length of the friction path. The results of individual tests were given as an increase in the depth of the wear trace referenced to a single movement of the pin (nm/cycle). The movement cycle includes the movement of the pin between the extreme positions

3.3. Real conditions test rig and methods

The tests of the tribocorrosive wear of the chain wheel made of ADI containing Ni, Cu and Mo were carried out on a test rig designed especially for that purpose, which allowed reproducing the combined action of destructive factors typical of conveyors operated in tunnels or drifts in stone with a dry atmosphere (conditions of abrasive wear) or a wet atmosphere (conditions of tribocorrosive wear). A schematic diagram of the test rig is shown in Fig. 3, while the detailed methodology and the test rig itself were described in [36-38].

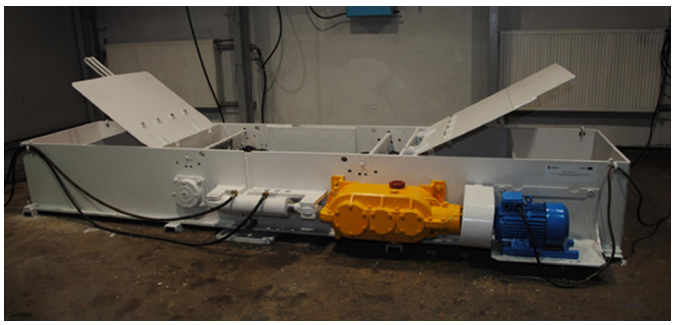

Fig. 3. The test rig for tribocorrosion tests in conditions reproducing the real operating conditions of the chain wheels

As a part of the tests, two variants of wear have been tested:

– in the presence of dry quartz abrasive,
– in the presence of a mixture of quartz abrasive and 3.5% NaCl solution in water.

The first variant of wear was realized by filling the box of the test rig with dry abrasive (Fig. 4), which ensured its presence in the area of mating between the chain wheel and the chain. The second variant of wear was realized by filling the box of the test rig with quartz abrasive and adding appropriate quantity of 3.5% salt solution in water.

Fig. 4. A view of the chain wheels during the wear tests in the presence of the quartz abrasive

The initial share of the corrosive agent in the abrasive was determined by dosing 900 kg of washed quartz sand with the original grain size of 1 mm, and then adding 100 litres of salt solution, which ensured its 10% share during the wear tests. In the course of the operation of the test rig, an accelerated evaporation of water from the abrasive-corrosive mixture took place due to the friction of chain wheels and the chain against the abrasive. In order to prevent the possibility of operating the test rig with dried abrasive, 20 litres of water were added to the mixture every 2 hours, which restored its initial consistency (Fig. 5). However, at the end of the wear tests with a hydrated mixture of sand, a qualitative change in the consistency of this mixture was observed, which was caused by the fact that oxide layers being removed were present in it (Fig. 6).

Two identical chain wheels (Fig. 7) made of ADI_360 were used for the wear tests. One of them was used in the test with the abrasive only, while the second was tested in conditions of combined action of the abrasive and the salt solution.

During the tests, a uniform, constant chain tension was applied, which ensured proper operation of the system without excessive dynamic loads from so-called "flogging" with a loose chain. At a fixed chain tension induced by the extension of the hydraulic cylinder, the total power consumed by both motors was 15 kW.

Fig. 5. A view of the test rig for wear tests filled with the abrasive mixture composed of quartz sand and water – at the initial stage of the tribocorrosive wear tests

Fig. 6. A view of the test rig for wear tests filled with the abrasive mixture composed of quartz sand and water – at the final stage of the tribocorrosive wear tests

The main wear tests in the presence of loose quartz abrasive and the abrasive containing the salt solution lasted 200 hours in total. For each direction of rotations, the wear tests lasted 100 hours, which corresponds to $1.19 \cdot 10^6$ cycles of mating between the chain seat and the chain (up to 4 contacts occur during 1 rotation).

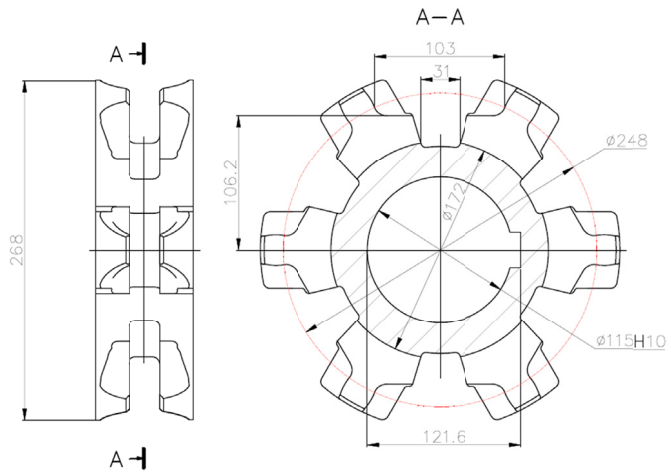

Fig. 7. A view of the chain wheel used for the wear testing

The averaged value of the maximum cavity in the surface of the chain wheel seat δ_{AVR_MAX} was adopted as the measure characterizing the abrasive wear. In order to determine this parameter before and after the wear tests, 24 mating surfaces between the chain wheel and the chain were measured with the use of Zeiss Acura measuring machine. Approx. 300 points along the predefined route of the measuring head of the machine were read and recorded during the measurement.

For each point of the route, the difference in the δ_i position was determined according to the formula:

$$\delta_i = \sqrt{\left(x_{i,1} - x_{i,2}\right)^2 + \left(y_{i,1} - y_{i,2}\right)^2 + \left(z_{i,1} - z_{i,2}\right)^2} \qquad (13)$$

where:

$x_{i,1}$ – x coordinate of the i-th point before the test,
$x_{i,2}$ – x coordinate of the i-th point after the test,
$y_{i,1}$ – y coordinate of the i-th point before the test,
$y_{i,2}$ – y coordinate of the i-th point after the test,
$z_{i,1}$ – z coordinate of the i-th point before the test,
$z_{i,2}$ – z coordinate of the i-th point after the test.

Then, for the calculated values of δ_i, the value of the maximum cavity in the surface of the chain wheel seat δ_{i_MAX} and the averaged value δ_{AVR_MAX} were determined [12,13].

4. Results and discussion

4.1. Results of the laboratory test

The resistance of ADI_360 to the impact of a corrosive environment was evaluated based on:

– polarization curves in the cathodic and anodic areas,
– changes in the corrosion potential E_{cor} as a function of time.

These methods were applied for static conditions (sample immersed in electrolyte) and during the wear test (counter- sample is sliding against the surface of the sample in the presence of electrolyte). The results obtained are shown in Fig. 8. The plots of the polarization curves do not indicate the occurrence of an area of passivation [32,33]. A distinct decrease in the corrosion potential proves that the ADI corrodes in 3.5% NaCl solution. Fig. 9 illustrates an intensification of the corrosive impacts in frictional conditions [34,35]. Based on the polarization curves, the corrosion potential E_{cor} and the corrosion current density (I_{cor}) were determined using the method of Tafel equations. The results of the analyses are presented in Table 4. Using the Faraday equation for the corrosion current density, the rate of corrosion was also determined. When friction occurs, the corrosion current density (loss of material) increases threefold.

The main wear tests were performed in order to assess:

– material loss V_t caused by the simultaneous mechanical and corrosive impacts – at a free corrosion potential,
– material loss V_f caused exclusively by mechanical impacts – in the presence of electrolyte at cathodic polarization –800 mV (SCE).

TABLE 4

The corrosion potential E_{cor} and the corrosion current density I_{cor} of ADI in 3.5% NaCl solution

Tests conditions	Tests conditions	Corrosion potential E_{cor}, mV$_{(SCE)}$	Corrosion current density i_{cor}, µA/cm^2
Stationary	–580	184	0,07
Wear test	–649	576	0,20

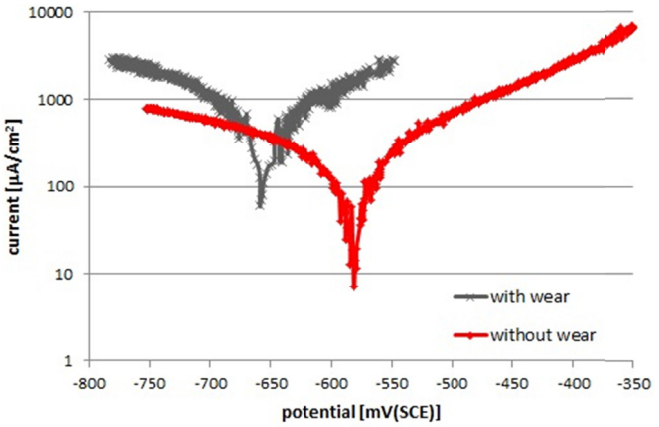

Fig. 8. ADI polarization curves in 3.5% NaCl solution (2 mV/s)

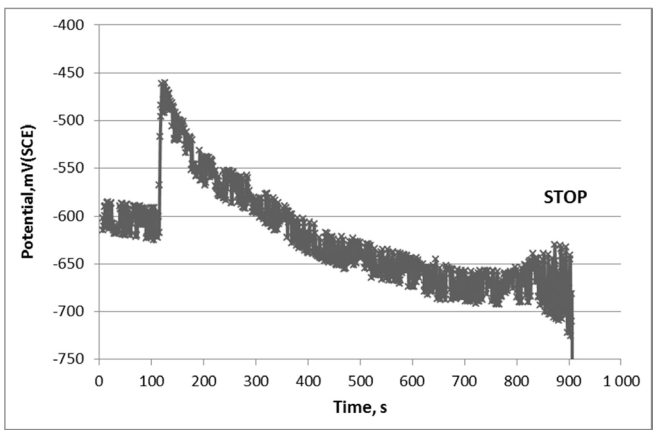

Fig. 9. Change in the corrosion potential of ADI in 3.5% NaCl solution during the test

Tables 5 and 6 present the test results as well as the results of the selection of components for laboratory tests.

TABLE 5

Results of laboratory tests of the wear of ADI in 3.5% NaCl solution

Wear parameter	Value, nm/cycle	Method of determining
Total wear, V_t	0,093	Direct measurement
Wear caused by friction (without participation of corrosion), V_f	0,056	Direct measurement
Wear caused exclusively by corrosion, V_{cor}	0,007	Estimation based on $i_{cor\_without\_wear}$
The total value of the wear component resulting from the corrosive impact and the increase in wear caused by the synergistic effect of friction on corrosion, $V_{cor} + \Delta V_{cor}$	0,020	Estimation based on $i_{cor\_with\_wear}$
The increase in the wear resulting from the synergistic effect of friction on corrosion, ΔV_{cor}	0,013	Equation (5)
The increase in the wear resulting from the synergistic effect of corrosion on friction, ΔV_f	0,017	Equation (4)
Summary effect of the synergy of friction and corrosion ΔV	0,030	Equation (2)

TABLE 6

The synergistic components of wear of ADI_360 in 3.5% NaCl solution (expressed as percentage) in relation to the total wear V_t determined for laboratory tests

V_f/V_t	60,2%
V_{cor}/V_t	7,5%
$\Delta V/V_t$	32,3%
$\Delta V_f/V_t$	18,3%
$\Delta V_{cor}/V_t$	14,0%

After completion of the tests, the hardness was measured at the bottom of wear traces of the ADI_360 test sample. It was found that the surface hardness increased up to 550 HV in relation to the core hardness of 300 HV. The increase in hardness is associated with the transformation of a part of the blocky austenite into martensite.

In addition, microscopic observations were performed (Fig. 10) for both variants of the test (only mechanical wear and tribocorrosive wear) in the zone of contact between the sample and the counter-sample.

4.2. The results of the test in real operating conditions

During the wear tests, it sometimes happened that the area of mating between the wheel and the link chain was filled with quartz abrasive only and sometimes with a mixture of quartz abrasive and salt solution. As a result of the rotation of the chain wheel, a partial rotation of chain links took place, which resulted in movement of abrasive grains in the area of mating between the wheel and the chain. The movement of the abrasive was accompanied by micro-cutting of the wheel surface. Simultaneously with the abrasive processes, the grains were also crushed.

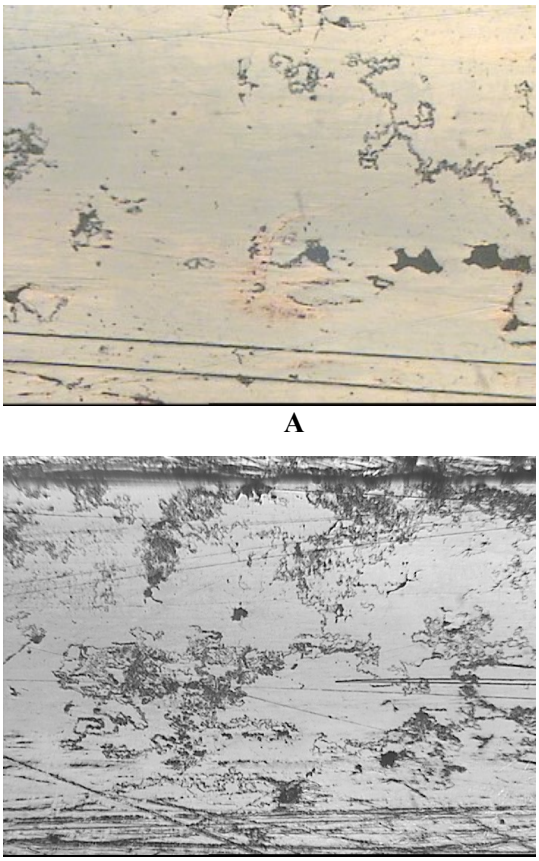

Fig. 10. A view of a trace surface: a) only mechanical wear – cathodic polarization, b) tribocorrosion (200×)

During 10 hours of operation of the test rig, the quartz sand grains were completely crushed. Despite a decrease in the size of the abrasive grains, an intensive abrasive wear was still observed. Due to the presence of water, a passivated oxygen layer was formed on the newly exposed surface by abrasive grains. It was easily removed by the diminished abrasive grains. Damage to the area of mating between the wheel and the chain had the form of shallow abrasions (Fig. 11).

The values of the maximum abrasive wear δ_{AVR_MAX} together with the measures of dispersion for the chain wheels tested in the presence of the abrasive only and in the presence of a mixture of abrasive and salt solution are listed in Table 7.

TABLE 7

The determined parameters characterizing the abrasive wear δ_{AVR_MAX} of ADI_360 for the materials considered; Cor – the variant involving the salt solution

Sample	δ_{AVR_MAX}, mm	S_δ, mm
ADI_360	0,934	0,057
ADI_360_Cor	1,406	0,072

When comparing the results of the wear in terms of the impact of the presence of a corrosive factor (water + 3.5% NaCl), it can easily be seen that values of wear for the variant of the tribocorrosive wear are higher. There was found a significant increase in the wear (by 50.5%) for the variant of the abrasive wear associated with the corrosive action of salt solution as compared with the variant of the abrasive wear in dry quartz abrasive.

Fig. 11. Traces of abrasions on tooth surfaces of the test chain wheels made of ADI_360; A – the variant of wear involving quartz abrasive, B – the variant of wear involving quartz abrasive and salt solution

After completion of the wear tests, samples for metallographic examinations were taken from a tooth of the chain wheel and then they were ground and polished. In order to determine the microstructure, the samples were etched with 3% Nital solution.

Fig. 12 shows the microstructure of ADI_360_COR chain wheel approx. 2 mm under the surface subjected to abrasive wear. The microstructure of the matrix is composed of upper ausferrite with a content of residual austenite at a level of approx. 40%. The graphite maintained its spherical shape, no deformation caused by the abrasive or by the pressure of the chain was found. Fig. 13 shows shallow cavities oriented askew in relation to the surface, caused by the action of the abrasive. At the surface the graphite was oriented almost in parallel to the surface, but in the near-surface zone it is characterized by an elongated shape, a complete lack of sphericity and the orientation at an angle of approx. 45 degrees in relation to the surface. A characteristic arrangement of the deformed graphite inclusions is associated with a non-rectilinear sliding movement of the chain in the area of mating with the chain wheel. The zone of the deformed graphite is located in the area of 0-0.2 mm under the surface of wear. The deformations of the graphite in the near-surface zone are shown in more detail in Fig. 14.

Fig. 15 shows the microstructure of the near-surface zone of the chain wheel subject to wear in tribocorrosive conditions. Relatively deep and extensive cavities with a triangular or trapezoidal cross section can be easily seen on the surface. These cavities were caused by the action of the quartz abrasive.

A characteristic feature for the structures shown in Fig. 15 is an apparent lack of graphite deformations. The spherical shape of the graphite was maintained even in the immediate vicinity of the cutting caused by the action of quartz grains. This may suggest a smaller energy intensity of the microcutting process in the near-surface layer in conditions of the combined effect of abrasive and corrosive factors. The easier penetration of the surface layer by abrasive grains might be caused by an intensive formation of oxide layers in corrosive conditions on newly exposed surfaces and by a less intensive process of the transition of the residual austenite into martensite. This process depends to a significant degree on the value of the tension in the contact layer. A reduction in the intensity of the TRIP process is proved by a reduction in the hardness of the near-surface layer after a period of operation (Fig. 16).

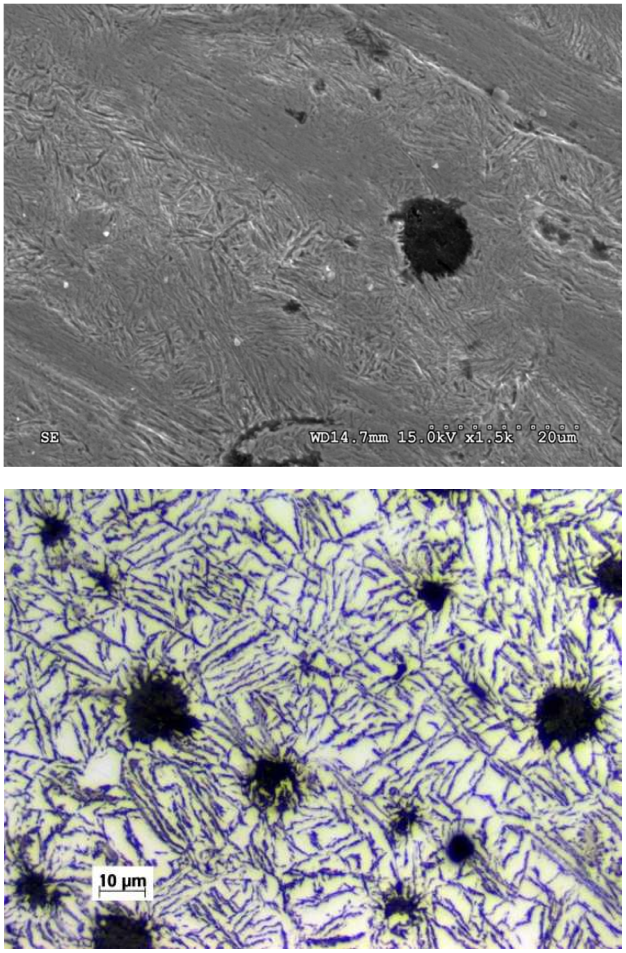

Fig. 12. The microstructure of ADI_360 in an area of approx. 2 mm under the surface subject to wear in abrasive conditions (lower figure – LM, upper figure – SEM)

Tables 8 and 9 present the test results as well as the results of the selection of components for operating tests. These results show clearly a synergistic effect accompanying the wear in tribocorrosive conditions. The wear of the cast iron in conditions

of the combined action of friction and corrosion is significantly higher than in the case of the elementary wear processes:

– caused exclusively by mechanical factors (friction) in the presence of electrolyte – wear process components (V_f and V_{ABR_f}),
– caused exclusively by corrosion in stationary electrolyte without frictional excitations – wear process components (V_{cor} and V_{ABR_cor}).

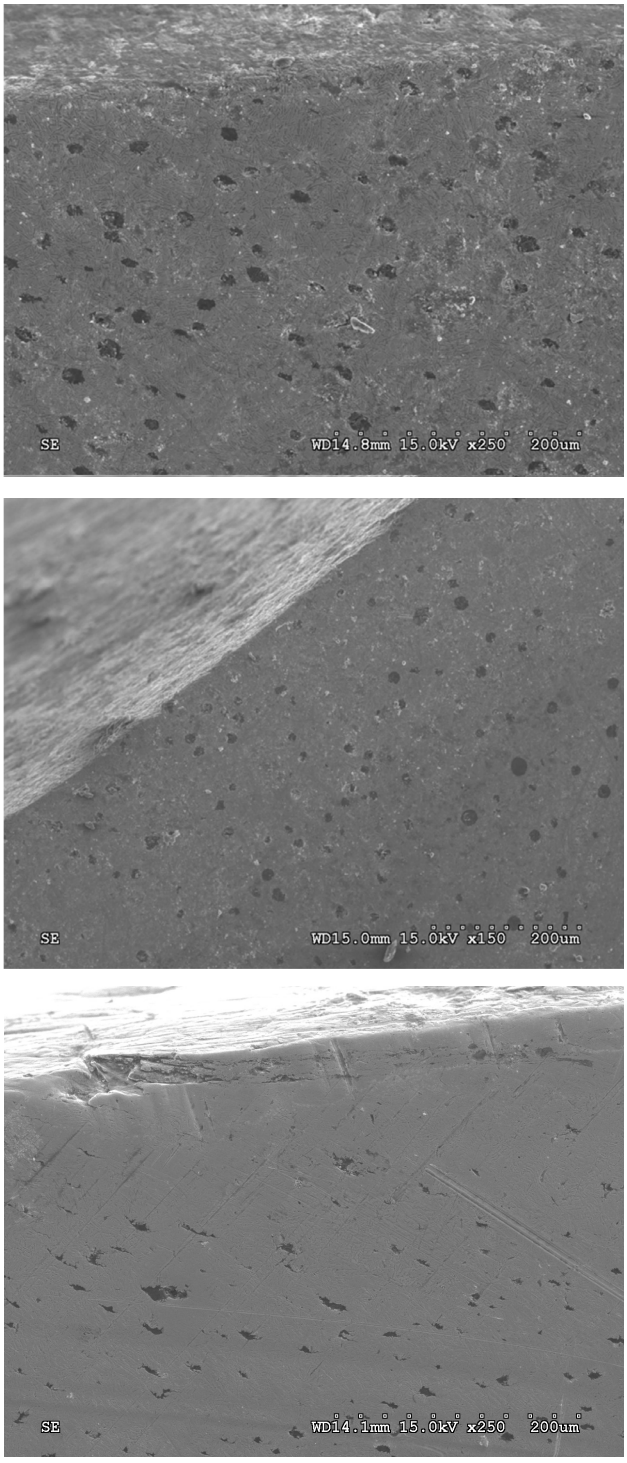

Fig. 13. The microstructure in an area of 0÷1 mm under the surface subject to wear in abrasive conditions; lower figure show microstructure of ADI_360, medium figure and upper figure shows microstructure of ADI_360_COR

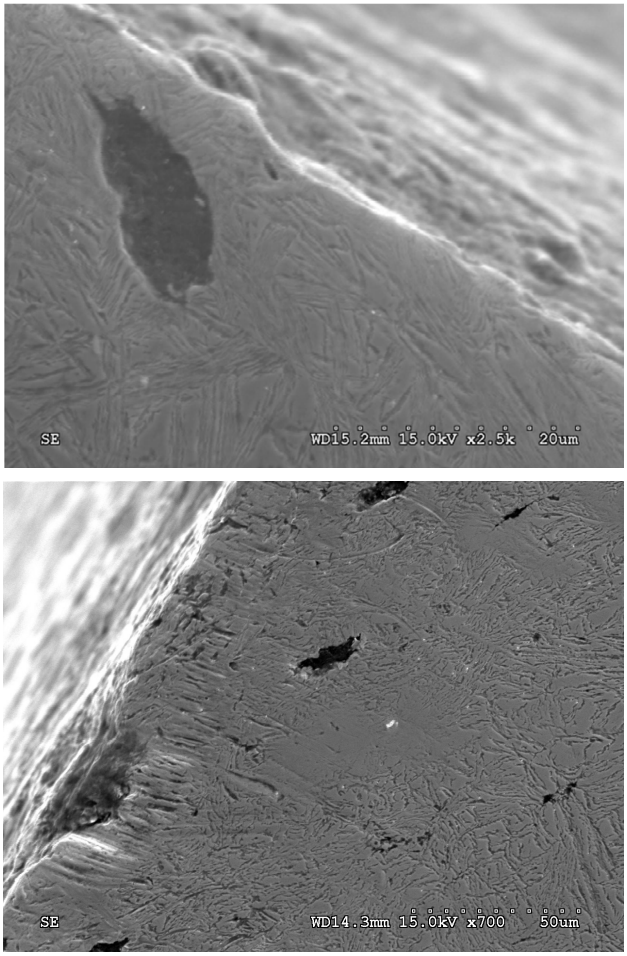

Fig. 14. Graphite nodules deformed as a result of the action of the abrasive in an area of approx. 0.05 mm under the Surface; lower figure show microstructure of ADI_360, upper figure show microstructure of ADI_360_COR

A quite high level of conformity can be seen between the results obtained for the laboratory tests and for the operating tests. The synergistic effect demonstrated for the laboratory conditions was determined at the level of 32.3%, while that for operating conditions – at the level of 32.8%.

The summary effect of the combined action of friction and corrosion (ΔV and ΔV_{ABR}) in a complex process of wear of case iron account for more than 30% of the total wear. On the one hand, this situation is caused by an intensification of corrosive effects in the friction pair, which is proved for example by the value of $\Delta V_{cor}/V_t = 43\%$. Such a course of electrochemical processes is confirmed by the characteristics shown in Fig. 8. On the other hand, corrosion also intensifies the mechanical wear of the cast iron tested. This is proved for example by the value of $\Delta V_f/V_t = 57\%$. This is caused probably by easier separation of the material in the structure affected by corrosion.

Faster removal of the material as a result of more intensive corrosion hinders the strengthening of near-surface layers of the ADI. The aforesaid strengthening may occur as a result of the transition of the residual austenite into martensite caused by the combined action of the abrasive and the chain pressure in the area of frictional contact [39-42]. Perhaps such a mechanism of

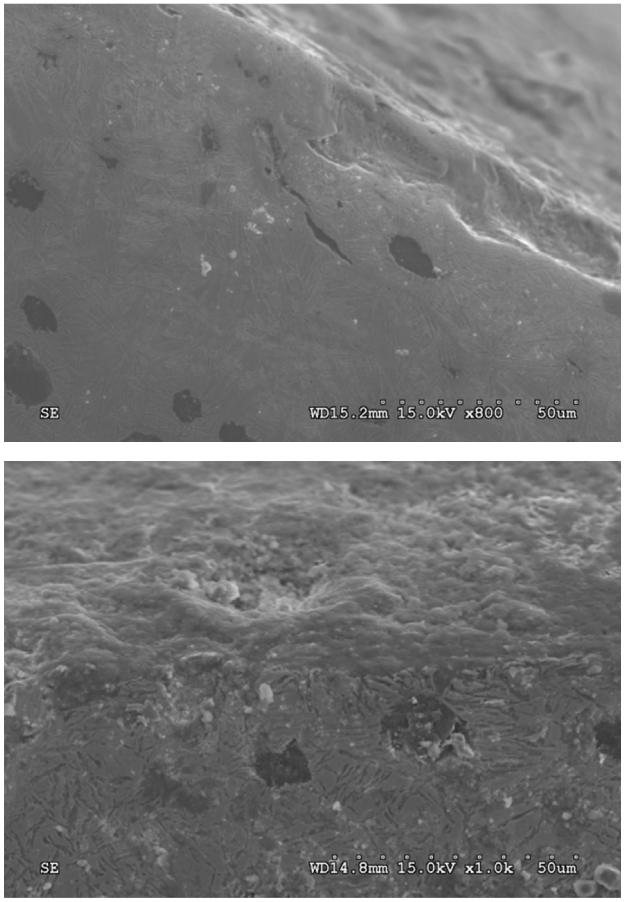

Fig. 15. Examples of the microstructure of the chain wheel made of the ADI_360_COR cast iron subject to wear in tribocorrosive conditions; lower figure – a view of an area of 0÷0.1 mm under the surface, upper figure – a fragment of the damaged surface with visible cutting caused by the action of the abrasive

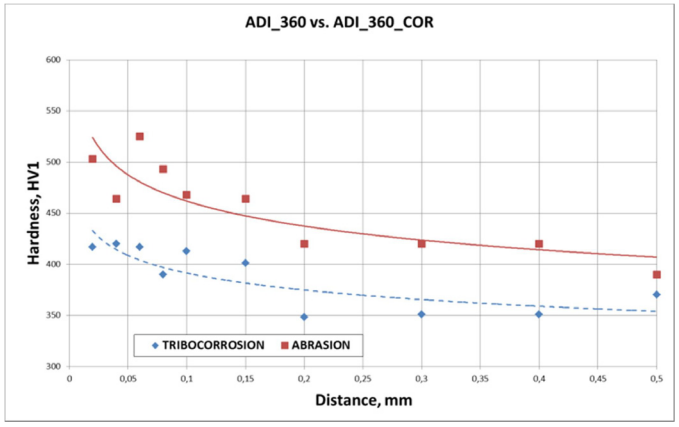

Fig. 16. The hardness HV0.1 of ADI_360 in an area of approx. 0.1 mm under the surface subject to wear in tribocorrosive conditions

change in the properties of near-surface layers is a reason that the wear of ADI_360 in 3.5% NaCl solution is significantly lower than that for steel with similar hardness. Earlier, the authors had conducted studies on tribocorrosion of AISI 304 corrosion-resistant steel. It has been found that in the case of this material (at a hardness of 300 HV) the intensity of the loss of material is 0.64 nm/cycle [31].

TABLE 8

Results of the operating tests of the wear of ADI_360 in 3.5% NaCl solution

Wear parameter	Value, nm/cycle	Method of determining
Total loss of material, $V_{ABR+COR}$	1,18	Direct measurement
Wear caused by frictional impact of the abrasive (without the participation of corrosion), V_{ABR_f}	0,786	Direct measurement
Corrosive wear in the presence of stationary abrasive and electrolyte, V_{ABR_cor}	0,0885	Equation (7)
The total value of the corrosive wear component in the presence of stationary abrasive and an increase in the wear as a result of the synergistic effect of the abrasive on corrosion, $(V_{ABR\_cor} + \Delta V_{ABR\_cor})$	0,250	Equation (9)
The increase in the wear resulting from the synergistic effect of the abrasive on corrosion, ΔV_{ABR_cor}	0,1615	Equation (10)
The increase in the wear resulting from the synergistic effect of corrosion products on the composition of the abrasive, ΔV_{ABR_f}	0,144	Equation (11)
Summary effect of the synergy of the action of the abrasive and corrosion, ΔV_{ABR}	0,3055	Equation (12)

TABLE 9

The synergistic components of the wear of ADI_360 in 3.5% NaCl solution (expressed as percentage) in relation to the value of the total loss of material $V_{ABR+COR}$ determined for the operating tests

$V_{ABR\_f}/V_{ABR+COR}$	66,6%
$V_{ABR\_cor}/V_{ABR+COR}$	7,5%
$\Delta V_{ABR}/V_{ABR+COR}$	25,89%
$\Delta V_{ABR\_f}/V_{ABR+COR}$	12,21%
$\Delta V_{ABR\_cor}/V_{ABR+COR}$	13,68%

5. Conclusions

1. The results presented in the paper indicate that in complex conditions of excitations, the wear of the cast iron tested depends to a large extent on the interaction of friction and corrosion. The effect of synergy account for more than 30% of the total loss of material.
2. In the analysed process the mechanical wear is intensified by corrosion, while the corrosive wear – by friction. The wear resistance in the complex conditions of excitations is therefore determined by a set of material properties (hardness and susceptibility to corrosion) associated with the structure of cast iron. Therefore, a significant advantage of the cast iron tested is its ability to strengthen as a result of the transition of residual austenite into martensite as a result of the effects occurring in the frictional contact zone.

3. The test results obtained on both the test rigs (the model test rig with a pin-on-plate pair and the test rig reproducing the real operating conditions) indicate similar relationships between the wear components of the cast iron tested. This may suggest that the degree of experimental identification of the wear process in terms of the influence of the excitations used on the intensity of the material loss is quite good.

Acknowledgements

The study was carried out as a part of the project "Innovative technology for production of tension members for transport systems with the use of cast materials", No. POIG.01.04.00-24-100/11 and "Development of the innovative technology of conveyor chutes routes using robotic methods", No. POIG.01.04.00-24-05-057 / 13.

REFERENCES

[1] A. Stachowiak, Tribocorrosion wear models in sliding pairs (Problemy modelowania zużywania tribokorozyjnego w układach ślizgowych). Wydawnictwo Naukowe Instytutu Technologii Eksploatacji – PIB, Radom, 2012.
[2] D. Landolt, Journal of Physics D: Applied Physics **39**, 3121-3127 (2006).
[3] A. Fischer, S. Mischler, Journal of Physics D: Applied Physics" **39**, 3128-3129 (2006).
[4] M.T. Mathew, P. Srinivasa Pai, R. Pourzal, A. Fischer, M.A. Wimmer, Advances in Tribology, 1-12, (2009)
[5] J.P. Celis, P. Ponthiaux, Wear **261**, 937-938 (2006).
[6] R.E.l. Noel, Ball A. Wear **87**, 351-361 (1983).
[7] A.W. Batchelor, G.E. Stachowiak, Wear **123**, 281-291 (1988).
[8] J. Spałek, The problems of engineering of machinery lubrication in mining (Problemy inżynierii smarowania maszyn w górnictwie). Wydawnictwo Politechniki Śląskiej, Gliwice 2003.
[9] A.N. Wieczorek, Management Systems in Production Engineering **17**, 28-34, (2015).
[10] R. Burdzik, P. Folęga, B. Łazarz, Z. Stanik, J. Warczek, Archives of Metallurgy and Materials **57**, 4, 987-993 (2012).
[11] M. Dolipski, T. Giza, S. Mikuła, P. Sobota, Bezpieczeństwo Pracy i Ochrona Środowiska w Górnictwie **12**, 3-8 (2011).
[12] K.L. Hayrynen, J.R. Keough, AFS Transactions **187**, 1-10, (2005).
[13] K.L. Hayrynen, J.R., Keough, G. L Pioszak, AFS Transactions, 1-15, (2010).
[14] J. Aranzabal, I. Gutierrez, J.M. Rodriguez-Ibabe, J.J. Urcola, Metalluragical and Materials Transactions **28a**, 1143-1156 (1997).
[15] J.M. Schissler, P. Brenot, J.P. Chobaut, , Mater. Sci. Tech. **5**, 71-77 (1987).
[16] A. Owhadi, J. Hedjazi, P. Davami, Mater. Sci. Tech. **14**, 245-250 (1998).
[17] D. Myszka, A.N. Wieczorek, Material Engineering (Inżynieria Materiałowa) **194**, 4, 332-335 (2013).
[18] D. Myszka, A.N. Wieczorek, Archives of Metallurgy and Materials **58**, 3, 967-970 (2013).
[19] N.D. Prasanna, M.K. Muralidhara, M.K. Agarwal, K. Radhakrishna, Transactions of 57th Indian Foundry Congress, 89-95 (2009).
[20] C.-H. Hsu, M.-L. Chen, Corrosion Science **52**, 2945-2949 (2010).
[21] A. Banerjee, P.K. Mitra, D.P. Chattopadhyay, A. Chowdhury, Transactions of 61st Indian Foundry Congress, 1-3 (2013).
[22] C.-H. Hsu, K.-T. Lin, Metallurgical And Materials Transactions **45A**, 1517-1523 (2014).
[23] Q.Z. Cai, B.K. Wei, Y. Tanaka, Acta Metallurgica Sinica **17**, 2, 122-130 (2004).
[24] H. Krawiec, J. Lelito, E. Tyrała, J. Banaś, Journal of Solid State Electrochemistry **13**, 6, 935-942 (2009).
[25] D. Myszka, M. Kłębczyk, A. Zych, L. Kwiatkowski, Archives of Foundry Engineering **9**, 1, 157-162 (2009).
[26] M.H. Hong, S.I. Pyun, Wear **147**, 59-67 (1991).
[27] T.C. Zhang, X.X. Jiang, S.Z. Li, X.C. Lu, Corrosion Science **36**, 12, 1953-1962 (1994).
[28] Y. Yahagi, Y. Mizutani, Wear **110**, 401-408 (1986).
[29] C. Hodge, M.M. Stack, Wear **270**, 104-114 (2010).
[30] A. Stachowiak, W. Zwierzycki, Tribology International **44**, 10, 1216-1224 (2011).
[31] A. Stachowiak, W. Zwierzycki, Wear **294**, 277-285 (2012).
[32] C.-H. Hsu, .J.-K. Lu, R.-J. Tsai, Surface & Coatings Technology **200**, 5725-5732 (2006).
[33] M. Salasi, G.B. Stachowiak, G.W. Stachowiak, Wear **271**, 1385-1396 (2011).
[34] Y. Sun, V. Rana, Materials Chemistry and Physics **129**, 138-147 (2011)
[35] M. Madej, Wear **317**, 179-187 (2014).
[36] A.N. Wieczorek, D. Myszka, J. Szromek, Biblioteka TEMAG **21**, 327-333 (2013).
[37] A.N. Wieczorek, Biblioteka TEMAG **22**, 277-285 (2013).
[38] A.N. Wieczorek, W. Polis, Management Systems in Production Engineering **19**, 175-178 (2015).
[39] D. Myszka, A.N. Wieczorek, Archives of Metallurgy and Materials **60**, 483-490 (2015).
[40] D. Myszka, L. Cybula, A.N. Wieczorek, Archives of Metallurgy and Materials **59**, 1181-1189 (2014).
[41] A.N. Wieczorek, Archives of Metallurgy and Materials **59**, 1665-1674 (2014).
[42] A.N. Wieczorek, Archives of Metallurgy and Materials **59**, 1675-1683 (2014).